

Discharge Coefficient Analysis for Sluice Gates Set in Weirs

Agostino Lauria^a, Antonino D’Ippolito^b, Francesco Calomino^c and Giancarlo Alfonsi^d
Department of Civil Engineering, Università della Calabria, Rende (CS), Italy

Keywords: Sluice Gates, Weir, Discharge Coefficients, Channel Inlet, CFD, RANS.

Abstract: Experimental tests and computational tests were performed to analyse discharge coefficients when gates are placed into weir walls. Gate slope and side contraction effect have been considered. A great number of experiments were conducted by considering three angles of inclination of the weir, three shape ratio and three values of the relative opening. Two mathematical equations were obtained, relating the discharge coefficient to the parameters that characterize the phenomenon. Furthermore, computational tests were performed following the Reynolds-Averaged Navier-Stokes (RANS) approach in conjunction with a turbulence closure model. In order to track the fluid surface, the Volume of Fluid algorithm being used. Numerical results have been validated against the experimental showing a good agreement. The validated numerical fluid flow can help to better understand the phenomenon not caught by the experiments.

1 INTRODUCTION

Sluice gates are efficient devices for flood control purposes and active defence against flooding. Despite sluice gates devices are commonly used, the hydraulic phenomena that occur their operation are not yet clear enough. Overall, the previous studies on sluice gates are not focused on the lateral contraction that can play a key role. By analysing the literature some experimental papers are present about sloping and vertical sluice gates (Montes, 1997, Sinniger and Hager, 1988). In the case of sluice gates forming an angle smaller than 90° with the horizontal plane, the discharge coefficient, C_d , decreased as the angle increased (Sinniger and Hager, 1988). The discharge coefficient decreases as the angle increases when this one is less than or equal to 90° (Gentilini, 1941). Other experimental works shows how the values of C_d against the relative opening range between 0.64 and 0.48 and decrease with the relative gate opening (Roth and Hager, 1999, Rajaratnam, 1967). The authors carried out one of the most complete studies on the topic, by means of tests on a rectangular flume and scale effect analysis. The authors showed the presence of a ridge upstream to the gate, moreover,

they observed a recirculation zone upstream to the gate, affecting the contraction of the vein, and two oblique stationary waves at the channel inlet. In the numerical field, many researchers reported a state-of-art review on the potential flow theory-based model, where the problem is described by a two-dimensional, irrotational, inviscid flow (Fangmeier and Strelkoff 1968, Larock 1969, Belaud and Litrico 2008). Some researchers carried out numerical simulations to study C_d , the distribution of the flow pressure and the flow contraction past a sluice gate (Kim, 2007, Akoz, 2010). Recently the Volume of Fluid (VoF) algorithm (Hirt et al., 1981), coupled with the Reynolds-Averaged Navier-Stokes equations, were used in several simulations of sluice gate flow (Cassan and Belaud, 2012, Lauria et al. 2020). Phenomena occurring during the underflow of sluice gates placed in weirs are not properly investigated. In this work, the phenomenon of the side contraction and gate slope, that should affect the results in terms of C_d , have been considered.

^a <https://orcid.org/0000-0003-4608-3684>

^b <https://orcid.org/0000-0003-3265-2196>

^c <https://orcid.org/0000-0002-6103-180X>

^d <https://orcid.org/0000-0001-5510-6708>

2 MATERIALS AND METHODS

By considering the definition sketch (Figure 1), the discharge Q can be expressed as a function of θ , a , b , h , g (gravity), ρ (water density), ν (kinematic viscosity) and σ (surface tension):

$$F(Q, a, b, h, \theta, g, \rho, \nu, \sigma) = 0 \quad (1)$$

After assuming $Q = C_d ab(2gh)^{0.5}$, and by selecting, a , g and ρ as basic variables, by applying the Π theorem and by following the procedure reported in Lauria et al. (2020), one has:

$$C_d = (a/h, b/a, \theta) \quad (2)$$

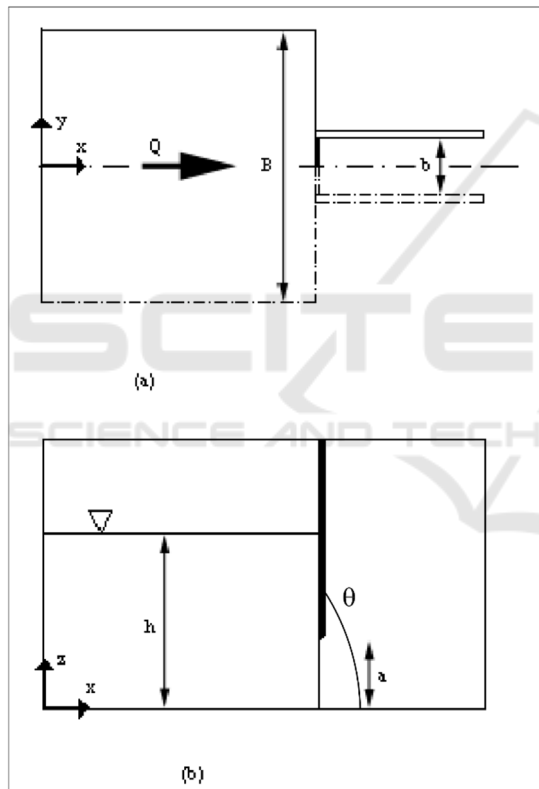


Figure 1: Definition sketch: (a) up and (b) lateral view.

2.1 Experimental Tests

Experimental campaigns were conducted in a physical model representing a structural device for flood control purposes (see Figure 2). In the model the weir is located into the riverbed causing a backwater effect, and consequently the storage of a flood volume in the upstream area (Lauria et al., 2020). The dimensions of the rectangular tank were

120 cm along the span-wise, 400 cm along the stream-wise, and 25 cm along the stream-normal direction. The weir physical model, 18 cm high and 120 cm wide, was placed at its downstream end. Vertical planes have been used to divide the weir in two parts and therefore create an orifice of dimension b (Lauria et al., 2020). A rectangular channel of width b was placed downstream of the gate opening (see Figure 1). Different values $b = 8,6, 10,6$ and $14,2$ cm (gate widths) has been considered. Experiments were conducted with different values of a (gate opening) and at different values of $\theta = 0,78, 1,11$ and $1,57$ rad (weir inclination) and at different values (see Table 1 in Lauria et al. 2020).

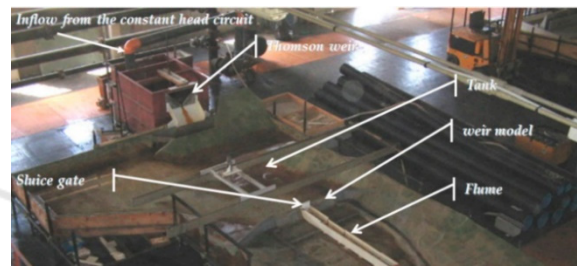


Figure 2: Downstream view of the physical model

The flow from the laboratory circuit fed the tank and the discharge values were collected by means of an ultrasonic flowmeter and by means of a Thomson weir (Figure 2). During experimental tests, the water level was measured by means of a pressure transducer and by means of an electric point gauge. The pressure measurements were obtained by means of a dedicated system able to get data in 12 different points of the tank (Lauria et al., 2020).

2.2 Numerical Simulations

To extending the investigation field computational tests were performed by solving the system of the three-dimensional Reynolds-averaged Navier-Stokes (RANS) equations, not reported here for brevity. A two – equation (Wilcox, 1998) turbulence closure model has been used. Reynolds stresses and the mean flow field has been related by means of the $k-\epsilon$ model (Lauder and Spalding, 1974). For the execution of the 27 tests chosen for the calculations (see Table 3 in Lauria et al., 2008), the Flow-3D[®] software has been used. The model equations, together with the turbulence model equations, are discretized with the finite-volume method (FVM). As for the discretization of the solution domain, a structured mesh has been built, where the dependent variables are stored at the centre of each cell space domain in a

co-located arrangement. To describe the free-surface behaviour the Volume of Fluid (VoF) method (Hirt, 1975) has been used. The algorithm has been used by other authors, always giving satisfactory results (see Alfonsi et al., 2012, 2013, 2015 and D'Ippolito et al., (2019)). The computational domain was composed by a three-dimensional geometry 49,6 cm along the streamwise direction and 40,0 cm along the spanwise direction and a rectangular one 30,0 cm along the stream-normal direction. The computing space dimensions spans respectively 79,6 cm along the streamwise 40,0 cm along the spanwise, and 30,0 cm along the stream-normal directions. The computational mesh was refined increasing points in all the directions. The considered mesh configuration was composed of about 1,9 million cells. Wall boundary condition was imposed at the bottom plane and at the model geometry. Symmetry boundary condition was imposed at the geometric symmetry plane and outflow conditions had been set on the $y-z$ end-plane of the computing domain. On the inflow section, the experimentally measured fluid depth has been set. As initial condition, experimentally measured fluid depth was set in the area of domain localized upstream of the gate. A multi-core computational system has been used for the computational runs (Alfonsi et al., 2012).

3 RESULTS AND DISCUSSION

Table 1 provides information about the experimental data, where different inclinations (θ) of the weir equal to 0,78 rad, 1,11 rad, and 1,57 rad, of the channel widths $b = 8,6, 10,6$ and $14,2$ cm, and of the gate opening $a = 5,0, 6,0$ and $7,0$ cm, were considered. The values of discharge coefficients as a function of a/h (relative opening) for the angle $\theta = 0,78, 1,11$ and $1,57$ rad (weir inclination), for $b/a = 1,23$ and $2,84$ (aspect ratio) and taking into account only the openings $a \geq 50$ mm, are shown in Figure 3. After identifying the value of the gate opening above which the role of viscosity is negligible a regression analysis was carried out using all the experimental data, and the following equation was obtained:

$$C_d = 0,388 * (a/h)^{-0,30} \theta^{0,06} \quad (3)$$

valid in the range $0,29 \leq a/h \leq 0,59$, $1,23 \leq b/a \leq 2,84$ and $0,78 \leq \theta \leq 1,57$ (in rad), with determination coefficient $R^2 = 0,97$.

Table 1: Laboratory tests.

θ (°)	a (mm)	b (mm)	h (mm)	Q (l/s)
45	50	86 - 142	109 - 125	3,4 - 5,2
45	60	86 - 142	136 - 144	4,2 - 7,2
45	70	86 - 142	125 - 145	4,8 - 7,4
63,4	50	86 - 142	131 - 149	3,6 - 6,3
63,4	60	86 - 142	145 - 156	4,3 - 7,6
63,4	70	86 - 142	129 - 153	5,1 - 7,4
90	50	86 - 142	142 - 176	4,2 - 7,4
90	60	86 - 142	149 - 152	4,8 - 7,7
90	70	86 - 142	122 - 180	4,9 - 7,6

Figure 4 shows the comparison between the numerical values of the computed discharge coefficients versus the observed ones, valid in the range $0,29 \leq a/h \leq 0,59$, $1,23 \leq b/a \leq 2,84$, for $\theta = 90^\circ$, and the results show a very good agreement. The validated numerical tool can help to investigate deeply the phenomena.

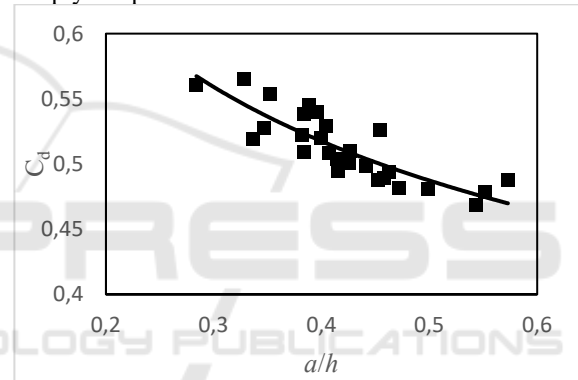


Figure 3: Experimental values of C_d versus a/h and regression line.

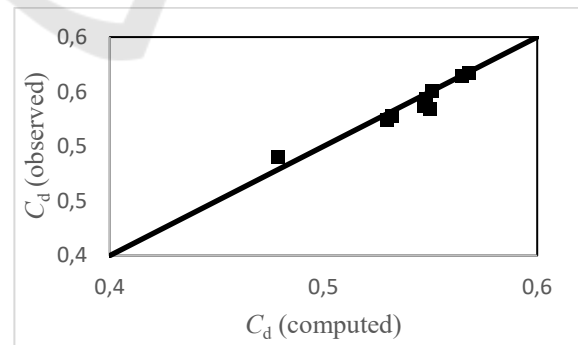


Figure 4: Numerically computed vs observed discharge coefficients for the case $\theta = 90^\circ$.

Considering the case $\theta = 45^\circ$, figure 5 shows the numerically computed discharge coefficients versus a/h . A regression analysis was carried out using the

numerical results, and the following equation was obtained:

$$C_d = 0,370 * (a/h)^{-0,356} \quad (4)$$

valid in the range $0,20 \leq a/h \leq 1,00$, $1,23 \leq b/a \leq 2,84$ and for $\theta = 45^\circ$, with determination coefficient $R^2 = 0,97$.

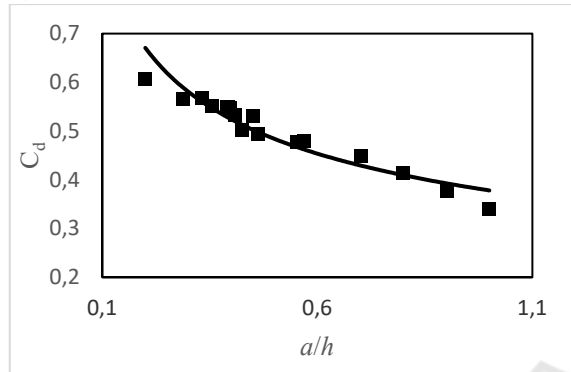


Figure 5: Numerical values of C_d versus a/h ($\theta = 45^\circ$).

4 CONCLUSIONS

Experimental tests and computational tests were performed to analyse discharge coefficients when gates are placed into weir walls. Gate slope and side contraction effect have been considered. Two mathematical equations have been obtained, relating the discharge coefficient to the parameters that characterize the phenomenon. The first one (equation (3)), was valid in the range $0,29 \leq a/h \leq 0,59$, $1,23 \leq b/a \leq 2,84$ and $0,78 \leq \theta \leq 1,57$ (with θ in rad). The second expression (equation (4)) is valid in a more extended range ($0,20 \leq a/h \leq 1,00$, $1,23 \leq b/a \leq 2,84$) and for $\theta = 45^\circ$. The proposed results and the validated numerical model, obtained by following a RANS approach, can help to better understand the phenomenon not caught by the experimental tests.

REFERENCES

- Montes, R., (1997). Irrotational flow and real fluid effects under planar sluice gates. *J. Hydraul. Eng.* 123, 219-232.
- Sinniger, R., Hager, W.H. (1988). *Constructions Hydrauliques. Ecoulements Stationnaires*; Presses Polytechniques Romandes; *Traité de Génie Civil de l'Ecole polytechnique fédérale de Lausanne*: Lausanne, Switzerland, Volume 15.
- Gentilini, B. (1941). Efflusso dalle luci soggiacenti alle paratoie piane inclinate e a settore. *L'Energia Elettrica*, 18, 361-380.
- Roth, A., Hager, W.H. (1999). Underflow of standard sluice gate. *Exp. Fluids*, 27, 339-350.
- Rajaratnam, N. (1977). Free flow immediately below sluice gates. *J. Hydraul. Div. ASCE*, 103, 345-351.
- Fangmeier D., Strelkoff T. (1968) Solution for gravity flow under a sluice gate. *J. Engrg. Mech. Div.* 94(EM1), 153-176.
- Larock B. (1969). Gravity-affected flow sluice gate. *J. Hydr. Div.* 95(HY4), 153-176.
- Belaud G., Litrico X. (2008). Closed-form solution of the potential flow in a contracted flume. *Journal of Fluid Mechanics* 599, 299-307.
- Kim D.G. (2007). Numerical analysis of free flow past a sluice gate. *KSCE Journal of Civil Engineering* 11, 127-132.
- Akoz M.S., Kirkgoz M.S., Oner A.A. (2010). Experimental and numerical modelling of a sluice gate flow. *Journal of Hydraulic Research* 47(2), 167-176.
- Hirt, C.W., Nichols, B.D. (1981). Volume of fluid (VOF) method for the dynamics of free boundaries. *J. Comput. Phys.*, 39, 201-225.
- Cassan L., Belaud G. (2012). Experimental and numerical investigation of flow under sluice gates. *Journal of Hydraulic Engineering* 138(4), 367-373.
- Lauria, A., Calomino, F., Alfonsi, G., D'Ippolito, A. (2020). Discharge coefficients for sluice gates set in weirs at different upstream wall inclinations. *Water* 2020, 12, 245.
- Wilcox, D.C. (1998). *Turbulence modelling for CFD*; DCW Industries: La Cañada, CA, USA.
- Lauder, B.E., Spalding, D.B. (1974). The numerical computation of turbulent flows. *Comput. Methods Appl. Mech. Eng.*, 3, 269-289.
- Alfonsi, G., Lauria, A., Primavera, L. (2012). Flow structures around a large-diameter circular cylinder. *J. Flow Visual. Image Process.*, 19(1), 15-35.
- Alfonsi, G., Lauria, A., Primavera, L. (2013). On evaluation of wave forces and runups on cylindrical obstacles. *J. Flow Visual. Image Process.*, 20, 269-291
- Alfonsi, G., Lauria, A., Primavera, L. (2015). The field of flow structures generated by a wave of viscous fluid around vertical circular cylinder piercing the free surface. *Procedia Eng.*, 116, 103-110.
- D'Ippolito, A., Lauria, A., Alfonsi, G., Calomino, F. (2019) Investigation of flow resistance exerted by rigid emergent vegetation in open channel. *Acta Geophys.*, 67, 971-986.
- Alfonsi, G., Lauria, A., Primavera, L. (2012). A study of the vortical structures past the lower portion of the Ahmed car model. *J. Flow Visual. Image Process.*, 19, 81-95.